DESCENT Analysis for Rotorcraft Survivability with Power Loss

Matthew W. Floros
Aerospace Engineer
US Army Research Laboratory
Hampton, Virginia
matt.floros@us.army.mil

Abstract

An analysis has been developed to model a rotorcraft with power loss. Partial power recovery to a flyaway condition, partial power landing, and autorotation to landing with a complete power loss are considered. An optimal control procedure is implemented to predict the pilot response to the power loss with the objective of minimizing the horizontal and vertical impact velocities in the case of a landing and achieving a sustainable steady state flight condition for flyaway. The physical and optimal control models are based on previous work, but have been extended with rate controls and additional constraints to more closely represent the pilot reaction and physics of the helicopter motion. The model is validated for autorotative landings from hover and forward flight initial conditions with data from a high energy rotor system flight test. With appropriate inputs to simulate the flight paths in the test data, good agreement is observed between the optimal control solutions and the test data. An example flyaway case is presented to illustrate the strengths and weaknesses of the current implementation.

Notation

A	rotor disk area
C_{d_0}	rotor blade minimum drag coefficient
C_T	rotor thrust coefficient
C_{T_0}	rotor initial thrust coefficient (weight)
$(C_T/\sigma)_s$	rotor stall thrust coefficient
D_x	vehicle horizontal drag
D_z	vehicle vertical drag
$\mathscr{F}$	optimal control integral part of objective function
$\mathscr{G}$	optimal control non-integral part of objective function
$\mathscr{J}$	optimal control objective function
$P_{k/d}$	Probability of kill given damage
Q	rotor torque
R	rotor radius
S	optimal control non-differential constraints
T	rotor thrust
U	optimal control control variable
$U_{()}$	optimal control slack control associated with $()$
W_x	optimal control velocity weighting factor
X	optimal control state variable
a	rotor blade lift curve slope
f	flat plate drag area
f_I, f_G	induced velocity and ground effect factors
g_0	acceleration due to gravity, non-dimensionalized by $\Omega_0 R^2$
n_s	rotor stall exponent
n_t	number of time steps in optimal control solution
v_{crit}	vertical impact velocity above which impact is considered an attrition
v_x, v_z	horizontal and vertical velocities
x, z	coordinate system horizontal and vertical directions and displacements (positive forward and down)
Ω_0	initial rotor speed
Π	optimal control scalar parameter
α	rotor disk angle
γ	rotor Lock number
λ	rotor inflow
μ	rotor advance ratio
ω	non-dimensional rotor speed
ρ	air density
σ	rotor solidity
τ	non-dimensional time ($= t\Omega_0$)
τ_f	non-dimensional terminal time ($= t_f\Omega_0$)
φ	optimal control differential constraints
ψ	optimal control end constraints
$()^\nabla$	differentiation with respect to normalized, non-dimensional time
$()^*$	differentiation with respect to non-dimensional time
$()_0, ()\|_0$	initial quantity
$()_1, ()\|_1$	final quantity
$\bar{()}$	scale factor, specifically for $\bar{X}$, $\bar{U}$, and $\bar{\Pi}$
$\hat{()}$	slack variable associated with $()$
$()_{\min}, ()_{\max}$	minimum and maximum values for a variable

Presented at the American Helicopter Society 65th Annual Forum, Grapevine, Texas, May 27–29, 2009.

Report Documentation Page

Form Approved
OMB No. 0704-0188

1. REPORT DATE	2. REPORT TYPE	3. DATES COVERED
MAY 2009		**00-00-2009 to 00-00-2009**

4. TITLE AND SUBTITLE	5a. CONTRACT NUMBER
DESCENT Analysis for Rotorcraft Survivability with Power Loss	5b. GRANT NUMBER
	5c. PROGRAM ELEMENT NUMBER
6. AUTHOR(S)	5d. PROJECT NUMBER
	5e. TASK NUMBER
	5f. WORK UNIT NUMBER
7. PERFORMING ORGANIZATION NAME(S) AND ADDRESS(ES) **US Army Research Laboratory,Hampton,VA,23681**	8. PERFORMING ORGANIZATION REPORT NUMBER
9. SPONSORING/MONITORING AGENCY NAME(S) AND ADDRESS(ES)	10. SPONSOR/MONITOR'S ACRONYM(S)
	11. SPONSOR/MONITOR'S REPORT NUMBER(S)

12. DISTRIBUTION/AVAILABILITY STATEMENT
Approved for public release; distribution unlimited

13. SUPPLEMENTARY NOTES

14. ABSTRACT
see report

15. SUBJECT TERMS

16. SECURITY CLASSIFICATION OF:			17. LIMITATION OF ABSTRACT	18. NUMBER OF PAGES	19a. NAME OF RESPONSIBLE PERSON
a. REPORT **unclassified**	b. ABSTRACT **unclassified**	c. THIS PAGE **unclassified**	**Same as Report (SAR)**	**14**	

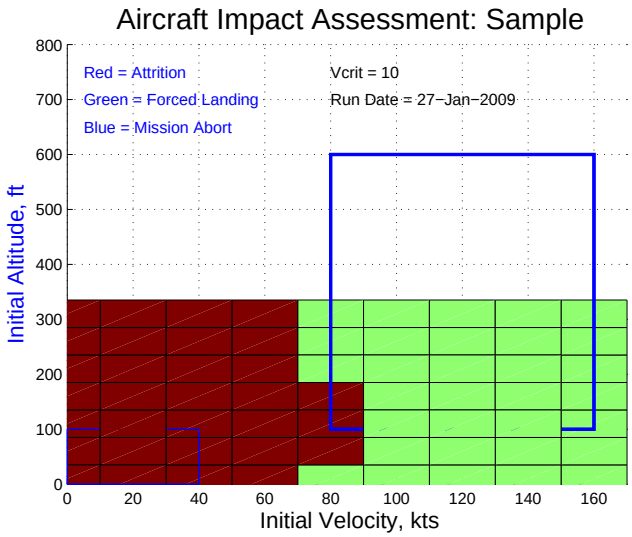

Fig. 1. Example $P_{k/d}$ plot for power off landing showing areas of attrition at low speed and forced landing at high speed.

Introduction

The purpose of the present work is to develop a tool to be used in assessing the survivability of rotorcraft with power loss. Specifically, given an initial altitude, forward speed, and power level, the tool is to determine if the helicopter can fly away or not, and if not, the level of damage that will result from the impact. The analysis is run over a range of altitude and forward speed and the results are collected into a probability of kill given damage or $P_{k/d}$. The $P_{k/d}$ indicates the likelihood of each type of kill for the failure within a range of altitude and forward speed.

Three kill types are considered. For a partial power loss, all three types of kill are possible. First, there is the potential for a *mission abort*, where the helicopter can fly away and return to a friendly base under its own power. If the helicopter is unable to fly away, it must descend to landing and potentially sustain additional damage. Only two levels of damage are considered for landings, namely *forced landing*, where the helicopter can be recovered, repaired, and returned to service, and *attrition,* where the vehicle is a total loss and is removed from the inventory. Clearly, for a complete power loss only the latter two kill types are possible. An example $P_{k/d}$ plot for power-off landing is shown in Figure 1.

Further objectives for the project were that it be computationally simple enough to run on a workstation computer and not require extensive mathematical or engineering knowledge of the user. Given those objectives, the effort is based upon and extends previous work from the 1970's and 1980's, where similar analysis was successfully implemented for hover (Ref. 1) and forward flight (Refs. 2, 3).

The previous work was modified and extended in several ways for the current effort. A basic departure was the choice of variables for the equations of motion. In references 1–3, the helicopter was controlled by thrust coefficients in the horizontal and vertical directions. For the current work, a single thrust coefficient and disk angle were used instead. The angle introduced nonlinear sine and cosine functions into the equations, but provided several advantages.

In the previous work, only a complete engine failure resulting in autorotation was addressed. The current effort includes partial power both for landings and mission abort flyaways.

Even with these changes, when exercised over a broad range of forward speeds and initial altitudes, beyond what was considered by the previous researchers, several deficiencies were revealed which resulted in optimal control paths which were not physically possible. These are addressed in the current work, mostly by additional constraints on the flight path, described later.

In this paper, a description of the initial model patterned after previous work is provided. Following that, the additional modifications, constraints and the justifications for them are provided.

Optimal Control Model

The bulk of the analysis is an optimal control procedure which calculates the pilot inputs and the resulting flight path from those inputs. The algorithm is called the Sequential Gradient-Restoration Algorithm (Ref. 4). In the algorithm, an optimal path is found to minimize an objective function, consisting of an integral portion, $\mathscr{F}$ and a non-integral portion $\mathscr{G}$. The solution is subject to differential constraints φ, non-differential constraints S, and end constraints ψ over a unit length of time. The constraints are specified in equations that sum to zero when the constraint is met. If the equation is nonzero, the value is constraint error. The algorithm operates on state variables, control variables, and scalar variables to reduce constraint error to zero and to minimize the objective function as much as possible. It is general purpose and then entire problem is defined by the variables described above.

Each state and control variable is a vector of length n_t. The scalar parameters are values which are variable but do not change with time. For the present application, the only scalar parameter is τ, which is the scale factor between the unit optimization interval and the non-dimensionalized time. Reference 4 provides an extremely detailed description of the algorithm and example problems with tabulated data to verify that the algorithm is implemented correctly. Only enough explanation is provided here to provide context for the application of the algorithm to the rotorcraft descent problem.

Like its name, the algorithm has two distinct phases, the gradient phase and the restoration phase. In the gra-

dient phase, the solution is modified to reduce the objective function. In the restoration phase, the constraint error is minimized until it is near zero within a specified tolerance. For example, the initial conditions for certain parameters may be simple expressions like a linear variation that does not satisfy the equations of motion. The restoration phase adjusts the variables until all of the constraints are satisfied. The gradient phase also introduces constraint error as it modifies the solution to minimize the objective function. So the solution alternates between gradient steps, which improve the objective function but introduce constraint errors, and restoration steps, which eliminate the constraint error.

To ensure a stable and converging solution, a limit is placed on how much error a gradient step can introduce. If an iteration step is calculated which results in too much error, the step is halved until the resulting error is within limits. Additionally, the objective function is evaluated *after restoration* to determine if the gradient step was successful. If the objective function is larger after restoration than the solution prior to the gradient step, the gradient step is halved until the resulting solution, after restoration, is improved.

Initially, the differential constraints represented equations of motion, the non-differential constraints were used to limit the controls, and a single scalar parameter was used to scale the time interval. However, additional constraints were required and increased the number of variables in the problem. A constraint on a control variable adds another control variable. A constraint on a state variable is more costly, adding both a control and a state variable.

Equations of Motion

The basic equations of motion for horizontal velocity, vertical velocity, and rotor speed, and the equations for rotor inflow are adapted from reference 1. The equations of motion are obtained from the sum of forces in the x and z directions and sum of torque about the rotor shaft. After modification to change the analysis variables from C_{T_x} and C_{T_z} to C_T and α as control variables, they are given in non-dimensional form by

$$\frac{d}{d\tau}v_z = g_0\left(1-\frac{C_T\cos\alpha}{C_{T_0}}\omega^2-\frac{(f/A)_z}{2C_{T_0}}v_z^2\right) \quad (1)$$

$$\frac{d}{d\tau}v_x = g_0\left(\frac{C_T\sin\alpha}{C_{T_0}}\omega^2-\frac{(f/A)_x}{2C_{T_0}}v_x^2\right) \quad (2)$$

$$\frac{d}{d\tau}\omega = -\frac{\gamma\omega^2}{a}\left\{\frac{C_{d_0}}{8}\left[1+\left(6\frac{C_T}{\sigma}\right)^2+\left(\frac{C_T/\sigma}{(C_T/\sigma)_s}\right)^{n_s}\right]\left[1+4.6\mu^2\right]+\frac{C_T}{\sigma}\lambda\right\} \quad (3)$$

$$\frac{d}{d\tau}z = v_z \quad (4)$$

The vertical force equilibrium in equation 1 is the sum of the weight (the equation is non-dimensionalized and normalized by C_{T_0}, so the 1 represents the weight), the vertical component of thrust, and the vertical drag of the fuselage. Note that the weight is positive while the thrust and drag terms are negative because the sign of z is positive down. Horizontal equilibrium in equation 2 is similar without the 1 representing non-dimensionalized weight.

The torque equilibrium in equation 3 is a sum of a semi-empirical expression for profile power and the momentum theory approximation of induced power. Of particular note is the third term in brackets. This term is intended to encourage the optimization algorithm to stay below stall by rapidly increasing torque above a specified stall thrust coefficient. A typical value for n_s is 20 or 30, so when the term in parentheses exceeds unity, the torque rises very quickly. Equation 4 is only needed to track altitude to determine when the helicopter reaches the ground.

For these equations, C_T and α are control variables, v_z, v_x, ω, and z are state variables, and the other variables are either specified or calculated from the states and controls. λ is calculated with corrections for vortex ring state and ground effect based on the horizontal and vertical speeds and the non-dimensional height above the ground.

The rotor induced velocity λ is assumed to be quasi-steady and is given by

$$\lambda = 1.15\lambda_{\text{hover}} f_I f_G \quad (5)$$

This equation is based on the hover induced velocity $\lambda_{\text{hover}}^2 = T/(2\rho A\Omega_0^2 R^2)$. The 1.15 factor is an analysis variable but is not normally modified. f_I and f_G are factors to correct for vortex ring state and ground effect. Like the equations of motion, they were taken from reference 1; they originally are found in references 5 and 6, respectively. Far from the ground and at normal airspeeds, both factors approach unity.

The inflow curve f_I has two expressions depending on the rotor state. A transcendental, but analytic momentum theory expression is used for normal forward flight. For nearly vertical flight, where momentum theory is not valid, an empirical expression for the vortex ring state is used. The equations are as follows:

$$f_I(\tilde{x},\tilde{z}) = \begin{cases} 1/(\sqrt{\tilde{z}^2+(\tilde{x}+f_I)^2}) & ,(2\tilde{x}+3)^2+\tilde{z}^2>1 \\ \tilde{x}(0.373\tilde{x}^2+0.598\tilde{z}^2-1.991) & ,(2\tilde{x}+3)^2+\tilde{z}^2\le 1 \end{cases} \quad (6)$$

The parameters $\tilde{x}$ and $\tilde{z}$ are normalized vertical and horizontal velocities,

$$\tilde{x} = \frac{\lambda_{\text{climb}}}{\lambda_{\text{hover}}} = \frac{v_x\sin\alpha - v_z\cos\alpha}{\lambda_{\text{hover}}\Omega_0 R} \quad (7)$$

$$\tilde{z} = \frac{\lambda_{\text{horiz}}}{\lambda_{\text{hover}}} = \frac{v_x \cos\alpha + v_z \sin\alpha}{\lambda_{\text{hover}} \Omega_0 R} \tag{8}$$

Ground effect is modeled with the expression

$$f_G = 1 - \frac{(-v_z + \lambda\cos\alpha)^2}{(-v_z + \lambda\cos\alpha)^2 + (v_x + \lambda\sin\alpha)^2} \frac{1}{(4z)^2} \tag{9}$$

where z is the non-dimensional rotor height above the ground. Note that the normal analysis variable z is the skid or wheel height, so z in the above expression must be corrected by the height of the rotor with the helicopter on the ground. Because ground effect is only significant near the ground, where z is small, the distinction is important.

Non-Dimensionalization and Scaling

The analysis operates on the equations in non-dimensionalized and scaled form. The non-dimensionalization follows standard convention for rotorcraft for the state variables. Additional scale factors are required for the optimal control procedure. The optimal control problem is well-scaled if similar changes in the variables produce similar changes in the objective function. For example, C_T is on the order of 0.005 whereas forward velocity, even non-dimensionalized by rotor speed may be 0.4. Scale factors are applied to bring the order of magnitude of each variable to approximately 1. The states, controls, and scalar parameter appear in the constraint equations, therefore, as $X/\bar{X}$, $U/\bar{U}$, $\Pi/\bar{\Pi}$. Though these factors are present in the code, for clarity, in this paper, equations are presented in non-dimensional form with this scaling already applied. The numerical values for the scale factors are given later when all of the states and controls have been defined.

The terminal time is τ_f, as yet unspecified. The optimal control algorithm operates on a specified interval from 0 to 1. So an additional normalization of the scaled, dimensionless time is required,

$$\xi = \frac{\tau}{\tau_f} \tag{10}$$

This ensures that the time variable the analysis uses ranges from 0 to 1. Because non-dimensionalization, a scale factor, and the normalization have been applied, differentiation and simply getting time in seconds from the unit time vector in the analysis can be confusing. The differential operators are given in terms of t, τ, and the single scalar scale factor $\bar{\Pi}_1$ by

$$(\,)^{\nabla} = \frac{d}{d\xi} = \tau_f \frac{d}{d\tau} = \frac{\tau_f}{\Omega_0 \bar{\Pi}_1} \frac{d}{dt} \tag{11}$$

In this paper, the equations are given in $\tau_f\,(d/d\tau)$ form since it is the easiest to understand. The computer implementation specifies equations in this form also, and applies the other scale factors in separate program units. Each of equations 1–4 therefore contain an additional τ_f factor in the code to reflect the $(\,)^{\nabla}$ differentiation. To obtain t in seconds from the unit interval time ξ,

$$t = \xi \frac{\tau}{\Omega_0 \bar{\Pi}_1} \tag{12}$$

For the remainder of the paper, the τ_f will be explicitly present as the additional differential equations are developed.

Table 1. State and control variables used in the baseline analysis

Variable	Symbol	Description
X_1	v_z	Vertical velocity
X_2	v_x	Horizontal velocity
X_3	ω	Rotor speed
X_4	z	Altitude
U_1	C_T	Rotor thrust coefficient
U_2	α	Disk plane angle

The analysis variables in terms of the state and control vectors X and U are given in Table 1. Additional state and control variables added as a result of the modifications to the baseline model are discussed below.

Implementation for Power Loss Application

The preceding discussion describes the math model and basic equations of motion for the helicopter in flight and represent only a slight departure from previous work. The remainder of the paper is the implementation and application of this analysis to the problem of descent or flyaway with power loss. The additional constraints for the problem and boundary values are discussed.

At several points in the course of development, it was observed that the optimal control algorithm would produce flight paths that violate physics but are well within the constraints of the analysis at that point. It is at the same time fascinating and frustrating to observe the innovative solutions that are produced when the analysis is unleashed on a wide range of initial conditions. It is fascinating because some solutions are not necessarily intuitive to a human analyst, yet are perfectly logical when the actual constraints or lack of constraints on the flight path are considered. But because the algorithm will only obey laws of physics when forced, each innovative yet impossible solution mandates a different approach or additional constraints on the problem and the attendant analysis and run time penalty associated with them.

Four modifications were made to the basic model and affect both controls and states. Initially, the analysis was for power off descent to landing only. Three changes were

implemented at that time: an altitude constraint, rate controls, and control limits. The last modification was for partial power, which was added in conjunction to the exit and end conditions discussed above. These four modifications are discussed below.

Altitude Constraint

The first modification to the analysis is the most amusing and serves as a good example to describe how state constraints are implemented in the analysis. The source of the problem was the observation that at high forward speed but low altitude initial conditions, the optimal flight path is for the helicopter to descend below ground level and ascend to the landing point to quickly decelerate and meet the zero altitude end condition. Because the analysis was only constrained to be zero at the final time, it was free to take on negative altitude elsewhere in the flight path. This behavior is replicated in nature when a bird approaches the edge of a building or a wire. It approaches slightly below the altitude of the landing spot and as it nears its target, ascends quickly to alight on the roof or wire with small horizontal and vertical speed. While it is encouraging that the flight path calculated by the algorithm is found in nature, it is not acceptable for the purposes of autorotative descent of a helicopter.

A constraint was added to force the analysis to keep the helicopter above ground prior to touchdown. The Sequential Gradient-Restoration algorithm operates on *equality* constraints, so some additional conversion is necessary to implement *inequality* constraints, such as $(z \geq 0)$. Each inequality constraint must be converted to an equality constraint in order to be implemented in the analysis. The process adds a control variable and an equality constraint to the analysis.

Initially, equation 4 tracks the vehicle altitude. Corrected for normalized time, the equation becomes

$$z^{\nabla} = \tau_f v_z \tag{13}$$

z is positive down, so it ranges from $(0 \leq z \leq z_f)$. So $z_0 = 0$ and z_f is equal to the initial altitude. The desired inequality constraint therefore is

$$z \leq z_f \tag{14}$$

This is converted to an equality constraint by using a slack variable $\hat{z}$:

$$z - z_f + \hat{z}^2 = 0 \tag{15}$$

Taking the derivative with respect to ξ,

$$\begin{aligned} z^{\nabla} + 2\hat{z}\hat{z}^{\nabla} &= 0 & (16)\\ \hat{z}^{\nabla} &= \tau_f U_z = \tau_f U_5 & (17) \end{aligned}$$

Now equation 13 is replaced with equation 17 in the equations of motion and the altitude is tracked through the slack variable $\hat{z}$ rather than z itself. Though generally not so, in this case because of the sign conventions, it is more convenient to track $\hat{z}$ since it is zero at τ_f, although it is initially $\sqrt{z_0}$ rather than z_0. Altitude is easily recovered through equation 15. After substituting equations 13 and 17 into equation 16, a non-differential equality constraint is is added to the S matrix as

$$v_z + 2\hat{z}U_z = 0 \tag{18}$$

A numerical problem arose as a result of equation 18 in the S matrix. Because the end constraint forces $\hat{z}$ to zero at the final time, at that time S becomes insensitive to U_z at that point. At times U_{z_f} would diverge to large values, causing the entire problem to be ill-conditioned. A static offset to $\hat{z}$ was applied so that the helicopter is instead constrained to remain above a slightly negative altitude. To an engineering approximation, this accomplishes the same purpose but avoids the numerical implementation issue.

The lower altitude bound need not be constant, it is only required to be a continuously differentiable function. A more rigorous method is envisioned where the bound on the inequality constraint is not constant but a line which crosses the x-axis between the τ_{n_t-1} and τ_f time steps. Such a constraint would ensure that the helicopter remains above the surface of the ground at all times except τ_f and at τ_f, U_z is a slightly negative number so a proper derivative for $S_{\hat{z}}$ can be calculated. Such an approach has not yet been implemented or tested.

Rate Controls

The approach of varying C_T and α as controls works well when the initial conditions for the optimal control are such that there is plenty of altitude and forward speed to perform the autorotative maneuver. However, for cases on the fringe and in regions of the altitude/velocity spectrum where a landing is not possible, many iterations are performed as the algorithm tries reduce the objective function as much as possible. In this case, often small variations in the controls are magnified. The C_T and α controls are discretized, merely a list of values at each of the n_t steps. There is nothing preventing large step changes in thrust or disk angle from one time step to the next, and these often occur as the landing task becomes more difficult.

Though thrust can vary relatively quickly, the pitch rate of the aircraft has a definite limit, so step changes in α are not realistic. Rate controls solve this problem. Rather than

controlling C_T and α directly, C_T^* and α^* are controlled and C_T and α become state variables. Step changes in C_T^* or α^* are smoothed by the integration operation. This conversion replaces the two controls and adds two additional states to the analysis. At the same time, each rate was limited by an inequality constraint, which added two additional controls and two additional non-differential constraints (one control and one constraint for each rate limit).

The thrust and pitch rates should vary from zero to a maximum rate (positive or negative). This can be written mathematically as

$$0 \leq (C_T^*)^2 \leq (C_{T\max}^*)^2 \tag{19}$$
$$0 \leq (\alpha^*)^2 \leq (\alpha_{\max}^*)^2 \tag{20}$$

The inequality constraints were converted to equality constraints in the same manner as described previously. The controls were implemented as $U_1 = C_T^*$ and $U_2 = \alpha^*$ being the controls for thrust rate and pitch rate, and U_3 and U_4 as the slack variables for the thrust and pitch rate limits, respectively. The resulting equations for the S matrix are

$$U_1^2 + U_3^2 - (C_{T\max}^*)^2 = 0 \tag{21}$$
$$U_2^2 + U_4^2 - (\alpha_{\max}^*)^2 = 0 \tag{22}$$

Additional state variables $X_5 = C_T$ and $X_6 = \alpha$ were added, resulting in additional differential constraints:

$$X_5^\nabla = C_T^\nabla = \tau_f C_T^* = \tau_f U_1 \tag{23}$$
$$X_6^\nabla = \alpha^\nabla = \tau_f \alpha^* = \tau_f U_2 \tag{24}$$

Even if the optimal control procedure prescribes a step change in C_T^* or α^*, the time histories for C_T and α are continuous.

Thrust Limiting

Although the torque equation (3) provides a penalty of rapidly increasing torque above a specified thrust, explicit constraints on thrust were still found to be necessary. Given unlimited thrust potential, the algorithm would produce control schedules which resulted in a C_T/σ greater than 0.2 and sometimes even 0.3 during a flare. The massive torque increase would rapidly slow the rotor below $0.5\Omega_0$ instantaneously rather than cause the optimal control to avoid such high thrust.

An explicit thrust limit was implemented in a similar manner to that for the altitude limit. In this case, though, independent upper and lower limits on thrust were desired to prevent the analysis from using negative thrust. Some careful crafting of the constraint equation provided both upper and lower limits on thrust with a single equation. The user inputs are the maximum and minimum thrust coefficients allowed for the helicopter. The maximum is unrelated to the stall thrust coefficient. It would normally be higher but can be the same or lower if that is desired by the user. An additional state X_7 and control U_6 are added as a result of the limit. The equality constraint is given by

$$\left(C_T - \frac{C_{T_{\min}} + C_{T\max}}{2}\right)^2 + \hat{C_T}^2 - \left(\frac{C_{T_{\min}} - C_{T\max}}{2}\right)^2 = 0 \tag{25}$$

Taking the derivative, the equality constraint is obtained

$$\left(C_T - \frac{C_{T_{\min}} + C_{T\max}}{2}\right) C_T^\nabla + \hat{C_T}\hat{C_T}^\nabla = 0 \tag{26}$$
$$\hat{C_T}^\nabla = \tau_f U_{\hat{C_T}} = \tau_f U_6 \tag{27}$$

and the expression for C_T^∇ is given in equation 23. Equation 26 becomes an additional non-differential constraint in the S matrix and equation 27 is an additional differential constraint in the φ matrix.

Partial Power

For a complete power loss, the torque expression in equation 3 is set equal to zero. For partial power, the engine can provide torque to the rotor. For a real engine, a control system or person adjusts the throttle to maintain rotor speed. If the torque available is not sufficient, the rotor speed will droop, but if excess torque is available, the control system will reduce fuel flow to maintain 100% RPM. This level of detail is not replicated in the current analysis. Rather, a maximum torque is known from user input. If the rotor demands more than the maximum available, rotor speed will droop like a real aircraft, but if excess torque is available, the algorithm can overspeed the rotor. A control variable Q_e ranging from 0 to the available torque specifies how much torque is applied to the rotor system. A second (slack) control variable U_{Q_e} is also required to convert the inequality constraint to an equality constraint.

For the partial power case, first equation 3 is modified to

$$\frac{d\omega}{d\tau} = -\frac{\gamma\omega^2}{a}\left\{-Q_e + \frac{C_{d_0}}{8}\left[1 + \left(6\frac{C_T}{\sigma}\right)^2 + \left(\frac{C_T/\sigma}{(C_T/\sigma)_s}\right)^{n_s}\right]\left[1 + 4.6\mu^2\right] + \frac{C_T}{\sigma}\lambda\right\} \tag{28}$$

The inequality constraint $0 \leq Q_e \leq Q_0$ is converted to an equality constraint for the S matrix given by

Table 2. State and control variables used in the complete analysis

Variable	Symbol	Description
X_1	v_z	Vertical velocity state
X_2	v_x	Horizontal velocity state
X_3	ω	Rotor speed state
X_4	$\hat{z}$	Slack variable (state) for altitude
X_5	C_T	Rotor thrust coefficient (state)
X_6	α	Disk plane angle state
X_7	$\hat{C_T}$	Slack variable (state) for C_T
U_1	C_T^*	Thrust rate control
U_2	α^*	Pitch rate control
U_3	$U_{C_T^*}$	Slack control for thrust rate limit
U_4	U_{α^*}	Slack control for pitch rate limit
U_5	U_z	Slack control for altitude
U_6	U_{C_T}	Slack control for thrust limit
U_7	Q_e	Engine torque control[a]
U_8	U_{Q_e}	Slack control for torque limit[a]

[a]Only present for partial power analysis

$$Q_e^2 + U_{Q_e}^2 - Q_0^2 = 0 \tag{29}$$

The complete set of states and controls is detailed in Table 2. When compared to Table 1, it is clear that to enforce limits on the problem, the size of the problem grows significantly. In its current state, hard limits exist on every control in the system and on some states. The original states v_z, v_x and ω remain unconstrained. The work in references 2 and 3 imposed a limit on vertical descent rate, but such a limit has not yet been found to be warranted. The nature of calculating the optimal path, possibly in combination with thrust and thrust rate limits, seems to prevent the analysis from allowing a high vertical sink rate. Verification and validation efforts in the future may reveal that a hard constraint on v_z is necessary, but results to date suggest it is more likely that ω will require limiting.

End Conditions and Initial Path

The optimal control operates on an initial path from the initial conditions (altitude, speed, and power available) to end conditions which depend on the power available. If sufficient power is available to fly away, the analysis attempts to calculate a flyaway path. If insufficient power to fly away is available or the flyaway path calculation fails, the a descent to landing is calculated. For each situation, an initial path must be supplied to the optimal control algorithm, preferably one that is close to the final path and satisfies the constraints. Obtaining an initial path close to the final path is difficult, after all, finding the final path is the purpose of the algorithm in the first place. But finding a path that meets or nearly meets the constraints is achievable.

First it is important to understand the initial conditions and end conditions before discussing the initial path between them. Only steady, level flight conditions at entry are currently used. The altitude, airspeed, and power available after the event completely define the initial state. The initial thrust coefficient and disk angle are calculated from the gross weight and initial speed. The end conditions differ for landing and mission abort flyaway, but are straightforward. They are implemented in a matrix, ψ which the optimal control algorithm forces to zero at the end of the time interval. Ideally, the initial path should result in $\psi = 0$ but this is not required and is not possible in some cases as discussed below.

For landing, the aircraft clearly must touch the ground, so the final altitude must be zero. In the current implementation, for a power-off landing, this is the only end criterion. For a partial power landing, an additional constraint is applied that the disk angle α must also be zero. This is based on an assumption that with partial power, the landing task is easier for the pilot and should be accomplished without dragging the tail on the ground.

For mission abort flyaway, the helicopter must be in level flight (zero sink rate), with rotor speed at 100%, and the forward velocity must be the minimum power speed. Mathematically these conditions are represented by

$$\psi_{\text{power off}} = \{\hat{z}\} \tag{30}$$

$$\psi_{\text{partial power}} = \begin{Bmatrix} \hat{z} \\ \alpha \end{Bmatrix} \tag{31}$$

$$\psi_{\text{flyaway}} = \begin{Bmatrix} \omega - 1 \\ v_z \\ v_x - \mu_{\text{opt}} \end{Bmatrix} \tag{32}$$

For descent to landing, the initial conditions are obtained by time integrating the equations of motion with a complete power loss and no change in controls. Without power, the helicopter cannot sustain steady level flight and descends to impact the ground. For a power off landing, the resulting flight path satisfies the constraint error to numerical precision so that the solution can proceed immediately to a gradient phase. For the partial power landing, the constraints are not completely met and a restoration is required to satisfy them.

Initial conditions for flyaway are in development. Assigning initial conditions in this case is not straightforward because there is not a discrete event such as striking the ground that can be reached by time integration. For flyaway, the pilot must transition from the flight condition at the power loss event to a condition where the helicopter can sustain level flight to escape without striking the ground. Beyond these criteria, there is no requirement to judge one flight path superior to another. If the end state of the flight path represents a steady flyaway condition, the analysis has succeeded in showing that the aircraft can fly away. Algorithmically, if the restoration satisfies the constraints in

equation 32, there is no need for gradient steps to improve the solution and the analysis exits.

But mathematically some initial conditions must be supplied to the algorithm to begin with, particularly the interval time τ_f. Several approaches have been investigated which work well in some instances but not others. The first is to use identical initial conditions to landing and simply let the restoration phase restore to a flyaway instead. This approach breaks down at very low altitude because the time interval to impact for a complete power loss is very short. If the flight condition is at very high or low speed and low altitude, the restoration phase cannot transition to the minimum power speed in such a short time.

A second option is to make all states constant, as though the helicopter continues flying with sufficient power available for a specified time. When the power is removed, the restoration procedure starts with a flight path that meets most of the constraints. Only the torque and $v_x - \mu_{\text{opt}}$ constraints are violated. It must then adjust the flight path to account for the torque loss and acceleration or deceleration. For this case, there is still the issue of determining a suitable analysis interval. τ_f should be short if the helicopter is already near the minimum power speed but longer if it is far above or below it. To account for this, the time required for a constant acceleration or deceleration to the minimum power speed is calculated. For example, if the initial speed is 100 knots and the minimum power speed is 80 knots, the time for a constant 0.2g deceleration from 100 to 80 knots is calculated and used for τ_f. This approach also works for some cases but not others. In particular, when the initial speed high, there is excess energy and the pilot should be able to gently decelerate in level flight to the minimum power speed while maintaining altitude, but this behavior is not always replicated by the analysis.

Objective Function and Exit Criteria

The purpose of optimal control algorithm, mathematically, is to minimize an objective function. The objective function consists of an integral part and a non-integral (scalar) part, $\mathscr{I} = \mathscr{F} + \mathscr{G}$. The most important physically is the non-integral part, given by

$$\mathscr{G} = v_{z_1}^2 + W_x v_{x_1}^2 \tag{33}$$

This represents a combination of the final vertical and horizontal components of velocity, scaled relative to each other by W_x. The scale factor determines the extent the optimal control procedure will work to minimize one term relative to the other. The terms are squared so that they are always positive.

The integral part is not strictly necessary, but has been implemented in order to *encourage* the algorithm rather than formally constraining it. The integral portion of the objective function is currently

$$\begin{aligned} \mathscr{F} &= 10(\omega - 1)^2(1 - \xi^4) \\ &\quad + (v_x - \mu_{\min})^2(1 - \cos 2\pi\xi) + v_z^2 \end{aligned} \tag{34}$$

The three terms are obtained from engineering judgment and observation of solutions the optimal control algorithm produces. The first term penalizes the objective function as the rotor speed deviates from 100% RPM. The $(1 - \xi^4)$ causes the penalty to go away at the end of the time interval where the rotor speed naturally drops during the flare. The second term encourages the algorithm to approach the minimum power speed. It also has a time factor so that the term diminishes to zero at the beginning and end of the time interval. This term is particularly important for descents starting from hover. The mathematics of the analysis see no difference between the helicopter going backward or forward from a hover initial condition. With this term, there is a mathematical reason to go forward. The final term penalizes the vertical velocity at all times in the time interval to provide further encouragement to the analysis to not build up an excessive sink rate.

As the optimal control algorithm minimizes the horizontal and vertical speeds at impact, a solution can be reached where further optimization of the flight path will not change the answer. The decision between an attrition and a forced landing is based solely on vertical impact velocity v_{crit}. Once the optimizer reduces the vertical impact velocity below v_{crit}, the landing is classified as a forced landing and further optimization is not necessary. In that case, if the horizontal velocity criterion $v_{x_1} \leq W_x v_{\text{crit}}$ has been met, the optimal control procedure exits and the analysis moves on to the next point. If the horizontal velocity criterion has not been met, the analysis continues until it is. The additional check on horizontal velocity is required to account for high forward speed with low initial altitude. In this case, the vertical sink rate may be less than v_{crit} after the initial restoration phase while the horizontal speed is very high. If v_x is not checked, the analysis exits at this point and incorrectly declares the point a forced landing. The additional v_x criterion prevents this exit and allows gradient phases to occur to minimize the horizontal velocity also.

The remaining two possible criteria normally result in an attrition because the optimal control algorithm is not able to reduce the impact velocity sufficiently and exits for one of two reasons. First, a rolling log of the objective function after each gradient iteration is also maintained. If the objective function has not been reduced by 1% in five gradient iterations (in other words, for iteration i, $\mathscr{I}_i < 0.99\mathscr{I}_{i-5}$), the optimal control considers the current solution to be optimal and exits. Alternatively, the code counts gradient iterations. If the number of gradient iterations exceeds a preset amount, the solution exits.

There is a third, defunct possibility for an unsuccessful exit from the optimal control. For any iterative procedure,

there is the possibility of a diverging solution. To address that situation gracefully, the constraint error is periodically checked for values of infinity or NaN (not a number). The constraint error is calculated from all of the variables in the analysis, so a non-numeric value in any variable naturally propagates to it. If such a value is detected, a flag is set which causes the analysis to "fall out" of any nested loops and move on to the next case.

Validation with Autorotation Data

Autorotation data from references 7 and 8 are used for validation of the power-off performance. The data are from a high inertia rotor test program where a helicopter was outfitted with additional tip weights to store more energy in the rotor. The effects of the additional energy on autorotation and abrupt maneuvers was then evaluated.

The test flights involved what the authors called "throttle chops," where the engine continues to run but is rapidly reduced to idle or near idle speed. A temporary provision was added to the DESCENT analysis to simulate this exponential decay in throttle by allowing the torque to decay from the pre-event level to a near zero level estimated from the test data. The optimal control normally uses all of the torque available to it when partial power is present, so the torque applied to the rotor in the simulation is similar to that in the test. Although achieving a successful landing in the analysis was straightforward, other inputs had to be modified to cause the flight path to landing to closely match the test data.

To obtain the appropriate torque parameters, the code was modified so that Q_e varies over the time interval. For equation 29, the constant Q_0 is replaced by a time-dependent $Q(\xi)$. Initially, it is equal to the (calculated) engine torque prior to the power loss. Reference 8 provides torque pressure data as a function of time. It is not reported how torque pressure in psi relates to torque in ft-lb, so Q_e was scaled so that that the ratio of initial torque to the final torque was the same as the ratio of the initial torque pressure to the idle torque pressure from the test data. For some cases the torque pressure at idle was nearly a third of the pressure prior to engine loss, and for others it was nearly zero.

The first case to be considered is the only forward flight case from reference 8. It is for the baseline rotor flying at 45 knots and 100 feet, although the test data indicate that the initial altitude is actually 114 feet. For this flight, the test data show that the helicopter lands at a relatively high horizontal speed of approximately 20–30 ft/sec but with almost no vertical speed. The landings were made to grass, and the authors describe the helicopter sliding to a stop in the grass after touchdown. To replicate this behavior, the weighting factor W_x was set to 0.05 and V_{crit} to 1 ft/sec. This allows a horizontal speed of up to 20 ft/sec at touchdown.

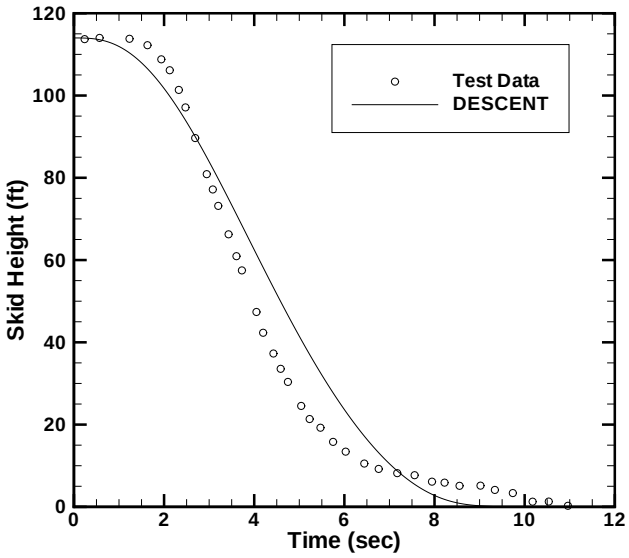

Fig. 2. Comparison of skid height from DESCENT analysis and Reference 8 for a modified OH-58A, 114 ft and 45 kt initial conditions.

The time histories of skid height, horizontal distance, and rotor speed are shown in Figures 2–4. The first item to verify is the length of the x-axis in the plots. As described earlier, in the DESCENT analysis, time is nondimensionalized by rotor speed and then normalized so that the optimal control performs its operations on a unit time interval. In addition, τ_f is scaled by $\bar{\Pi}_1$ in the computer program though those scale factors have been left out of the equations in this paper for simplicity. Considering all of that, although it seems trivial, it is quite important to verify that the time scale is correct. The optimal control response time is not exactly the same as the test data, but is clearly indicating seconds and not revolutions or some other scaled quantity. The analysis interval came out almost exactly the same with a W_x setting of 0.03, but the horizontal distance and landing speed were significantly higher in that case.

The altitude time histories (Figure 2) show similar trends, although the human pilot allows altitude to decrease more rapidly and then floats along the ground at about 10 feet for a few seconds before touching down. The optimal control descends gradually and touches down without floating.

The plots of horizontal distance, shown in Figure 3, are quite similar. The touchdown velocity (as indicated by the slope of the curve at touchdown) is about the same, though the DESCENT analysis touches down earlier. This value as well as the total distance traveled are strongly dependent on W_x. The exact values can't be "dialed in" with W_x because the optimal control works in discrete iterations and a single additional iteration may change the touchdown speed significantly.

Rotor speed is shown in Figure 4. Like the horizontal distance, the final rotor speed is consistent with the test

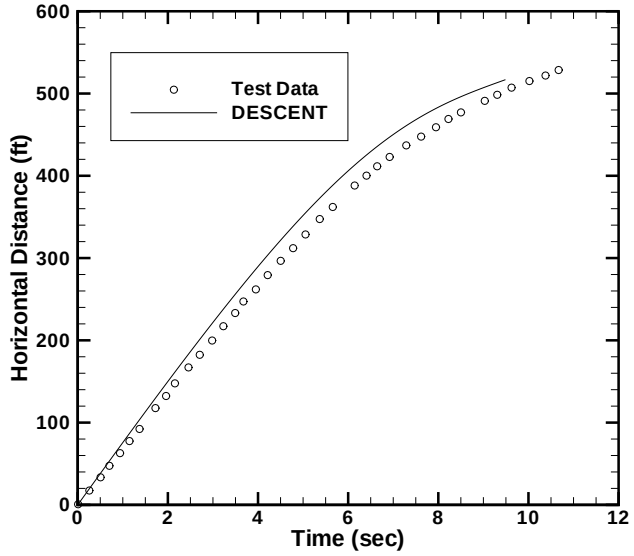

Fig. 3. Comparison of horizontal distance from DESCENT analysis and Reference 8 for a modified OH-58A, 114 ft and 45 kt initial conditions.

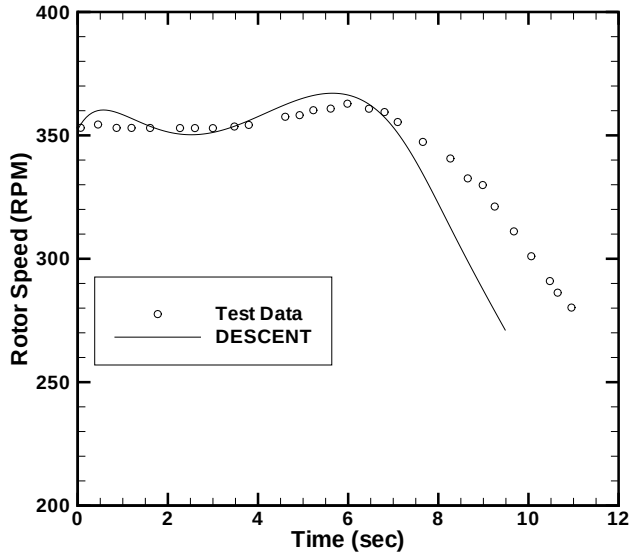

Fig. 4. Comparison of rotor speed from DESCENT analysis and Reference 8 for a modified OH-58A, 114 ft and 45 kt initial conditions.

data, despite the touchdown time being earlier. The decay of rotor speed is very sensitive to $C_{T_{\max}}$ and $(C_T/\sigma)_s$. Because of the rapid increase in torque with stall, the rotor speed can decay very quickly if the rotor is allowed to generate thrust significantly above stall. The analyst does not normally have the luxury of test data to adjust these parameters, but estimates of them should be known. The importance of these inputs is magnified when trying to match a specific flight path from test data. For normal operation of the analysis, a range of flight paths may be possible and only the impact velocity is subsequently used for the $P_{k/d}$

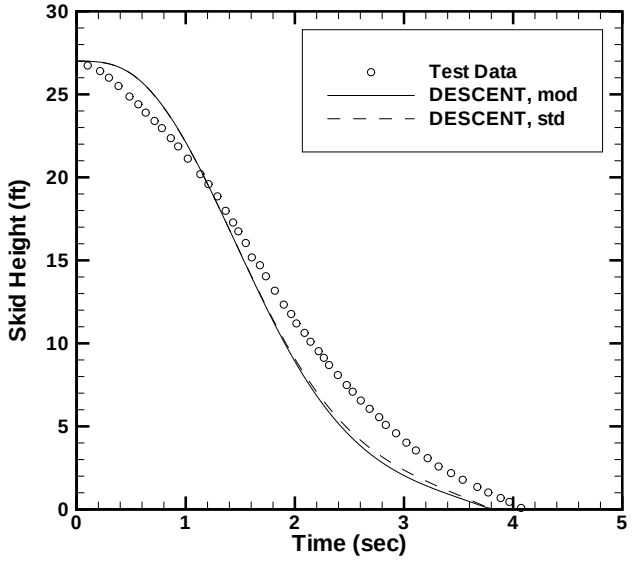

Fig. 5. Comparison of skid height from DESCENT analysis and Reference 8 for a modified OH-58A, 27-ft hover initial condition.

calculations.

The next case is a low hover case, where the helicopter starts from a hover at 27 feet at the time of the engine loss. For this case, the vertical impact velocity in the test data was estimated to be approximately 3 ft/sec, so v_{crit} was set to 2.5 ft/sec. If set to 3 ft/sec, the analysis calculates a pure vertical descent and does not enter the gradient phase at all. A vertical descent is perfectly reasonable, but a pilot would probably initiate some forward motion if for no other reason than to see where he was going.

However, the optimal control does not produce an answer with less than 2.5 ft/sec velocity without changing parameters. The reason is that the optimal control is trying to minimize both equations 33 and 34. It doesn't prioritize individual parts of the equations unless encouraged to do so by altering the relative magnitude of different terms. In order to match the test data, equation 34 was modified so that the v_x term was divided by 3. This encouraged the optimal control to place comparatively more emphasis on the impact velocities than forward velocity. Unmodified, intermediate solutions with impact speeds as low as 2.6 ft/sec are obtained, but the final solution after the program exits with 50 gradient iterations has an impact velocity of 3.05 ft/sec.

The results from both the modified and unmodified results are shown in Figures 5–7. The only plot where there is a significant difference is the horizontal distance, Figure 6. The DESCENT solutions are virtually identical for skid height and rotor speed.

The skid height profile, Figure 5, matches very closely between the test data and DESCENT calculation. Both the modified and standard DESCENT calculations are shown.

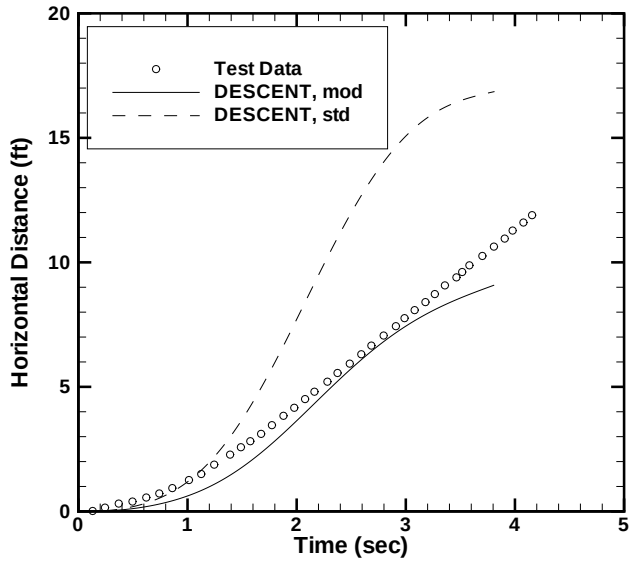

Fig. 6. Comparison of horizontal distance from DESCENT analysis and Reference 8 for a modified OH-58A, 27-ft hover initial condition.

The calculated flight times are slightly shorter, about 3.8 sec vs about 4.1 sec for the test data. Otherwise, the profiles are very similar. The slopes of the curves at touchdown are about the same, indicating that the 3 ft/sec approximation of impact velocity in the test data was accurate.

The horizontal distance profiles are shown in Figure 6. Here there are significant differences between the modified and standard DESCENT calculations. One difference between the calculations and test data is that the test pilot apparently made no attempt to decrease horizontal velocity at touchdown. The optimal control reduces horizontal velocity to 1.6 ft/sec in the modified case, and 1.0 ft/sec in the standard case. The modified case travels forward approximately 9 feet while the unmodified calculation is nearly 17. These bracket the test data, where the pilot advanced 12 feet. This illustrates the sensitivity of the optimal control to the objective function and the analysis parameters. So while it is difficult to get the calculations to quantitatively match the test data, it is clear from the time histories of skid height and rotor speed that the code is producing a qualitatively similar flight path.

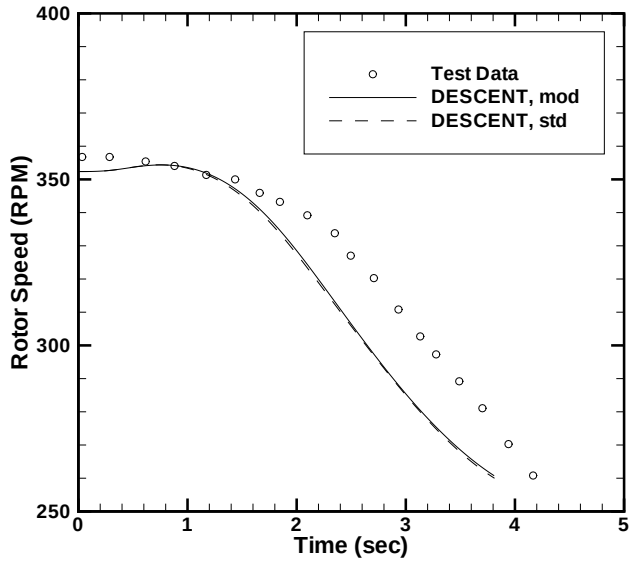

Fig. 7. Comparison of rotor speed from DESCENT analysis and Reference 8 for a modified OH-58A, 27-ft hover initial condition.

Rotor speed is shown in Figure 7. Like the skid height, the rotor speed is nearly identical for the two calculations. The calculated rotor speeds at touchdown are nearly identical to the test data, with only the slight time offset between the two. The profile is very similar. The rotor speed changes very little for a second or two and then the pilot starts the flare, bleeding off rotor speed much more quickly until touchdown.

The final case is a high hover case, where the helicopter starts at 100 feet. For this case, shown in Figure 17 of reference 8, the mid-inertia rotor is on the helicopter. The additional inertia causes more energy to be stored in the rotor. For the purposes of input, the only change to the helicopter model was changing the rotor inertia from 646 slug-ft^2 to 1100 slug-ft^2. For this comparison, no modification to the objective function was made in the DESCENT analysis.

The results, shown in Figures 8–10, are similar to those for the low hover case. The flight time is about one second shorter, 7 seconds vs 8 seconds for the test data. The calculated flight path has significantly more horizontal travel, but the rotor speed profile is similar. Like the other cases, flight paths with horizontal travel from as little as 40 feet to over 200 feet could be produced with small changes in the input.

In summary, while a direct numerical comparison is very difficult, a qualitative comparison shows that the analysis is reproducing the trends in the test data for both hover and forward flight initial conditions. The amount of energy being dissipated from the initial potential and kinetic energy of the helicopter in the analysis replicates the test because the velocities at the end of the flight are the same, and the rotor energy being dissipated is the same as shown by figures 4, 7, and 10. For the purposes of calculating Pk/d values, it is sufficient that the optimal control procedure approximates the energy management efforts of a human pilot.

Partial Power Flyaway

Although still in the development stage, the partial power flyaway functionality in DESCENT is mature enough to produce optimal control solutions. An example is presented here to illustrate the strengths and weaknesses of the current methodology. For this case, an engine loss at 100 feet altitude and 160 kts forward speed is simulated. After a single restoration phase, a flight path is produced where the

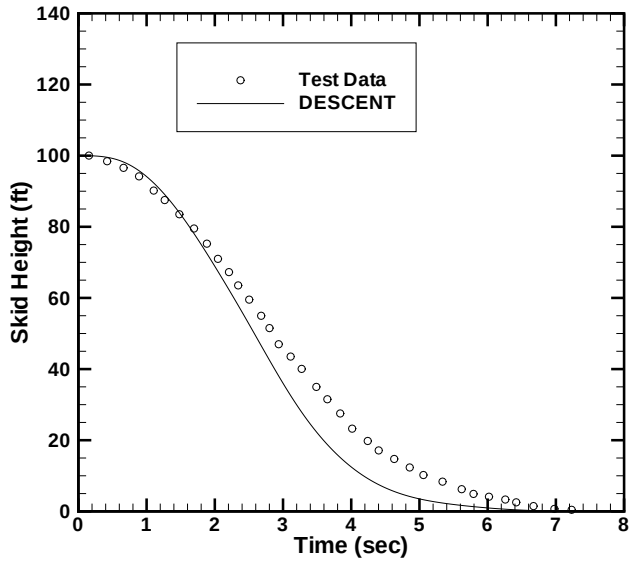

Fig. 8. Comparison of skid height from DESCENT analysis and Reference 8 for a modified OH-58A, 100-ft hover initial condition.

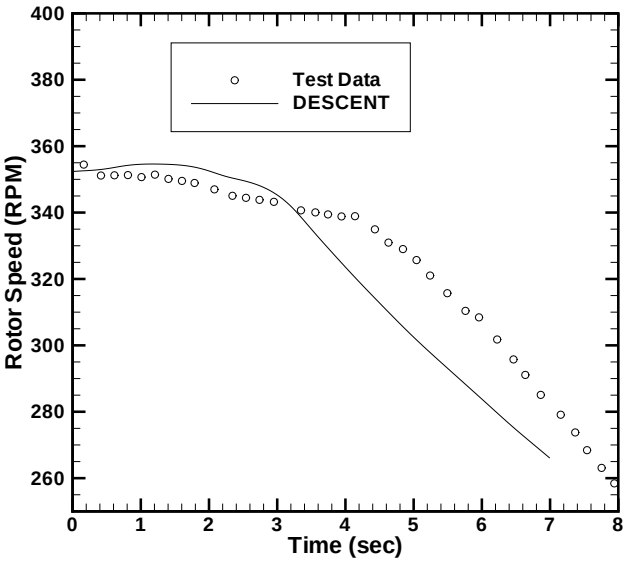

Fig. 10. Comparison of rotor speed from DESCENT analysis and Reference 8 for a modified OH-58A, 100-ft hover initial condition.

aircraft decelerates to the minimum power speed of approximately 80 kts in about 17 seconds, ending at 100% RPM and no sink rate as specified in equation 32. The airspeed is shown in Figure 11.

The controls are shown in Figure 12. Figure 12a shows the thrust controls while Figure 12b shows the pitch controls. In these plots, the rate controls are shown as solid lines and the resulting displacements are shown as dashed lines. The rate C_T^* initially increases the thrust coefficient to a high level and and near the end of the analysis decreases it

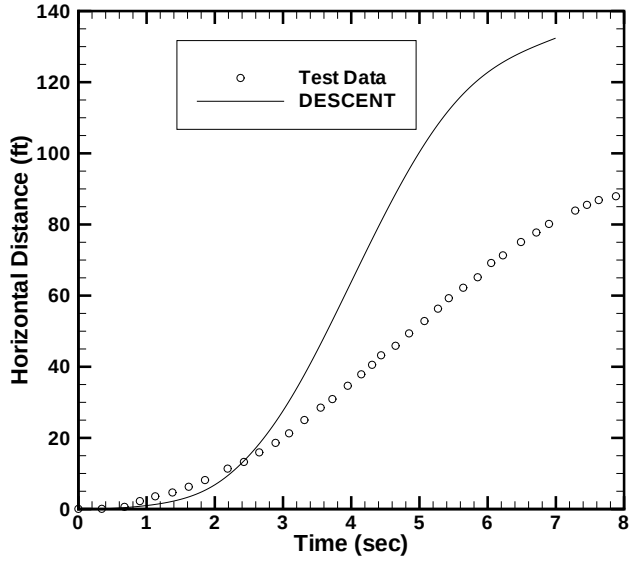

Fig. 9. Comparison of horizontal distance from DESCENT analysis and Reference 8 for a modified OH-58A, 100-ft hover initial condition.

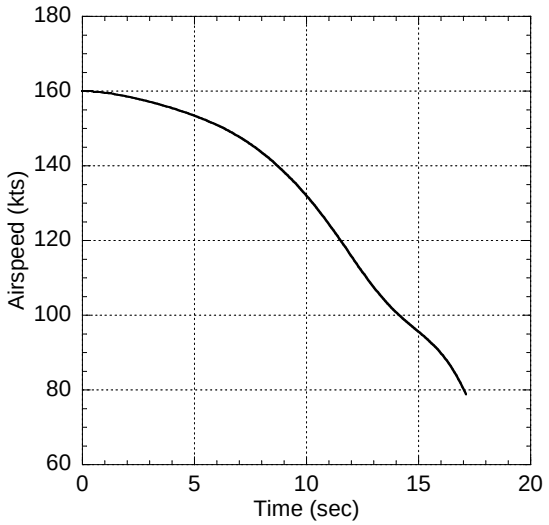

Fig. 11. Airspeed for partial power flyaway transition to minimum power speed.

slightly. For this case, the stall thrust coefficient $(C_T/\sigma)_s$ is 0.14, so it is exceeded, but only slightly. Meanwhile, the aircraft pitches back to about 20 deg nose up to achieve the rapid deceleration in Figure 11.

The effect on the sink rate and altitude is shown in Figure 13. Like the previous plots, the rate (v_z) is shown with a solid line and the displacement (altitude $\hat{z}$) is the dashed line. As the aircraft immediately pitches back and increases thrust, the sink rate is initially negative. As the helicopter bleeds off kinetic energy from the excess airspeed, it climbs from 100 to almost 140 feet and then abruptly drops to 110 feet and levels out. This flight path may seem erratic, but it

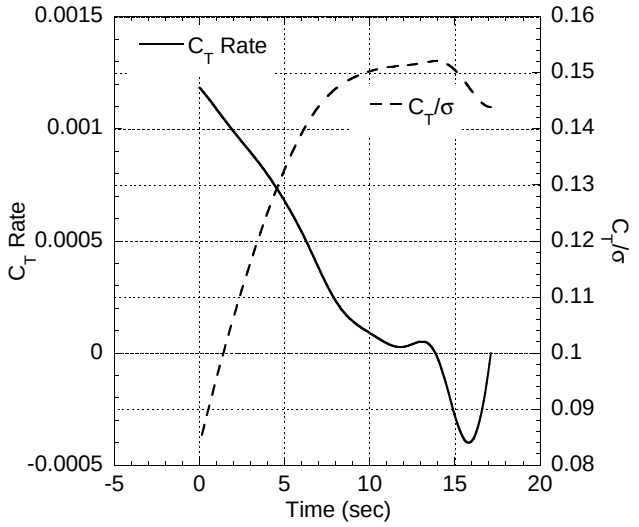

(a) Thrust Coefficient and Rate

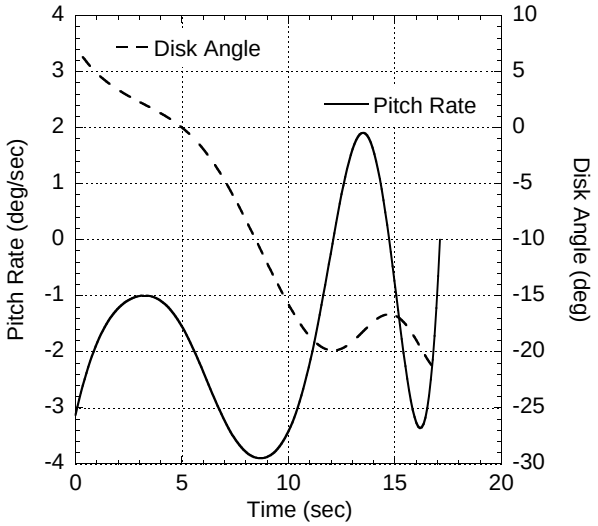

(b) Disk Angle and Pitch Rate

Fig. 12. Displacement and rate controls for thrust coefficient and disk angle for partial power flyaway transition to minimum power speed.

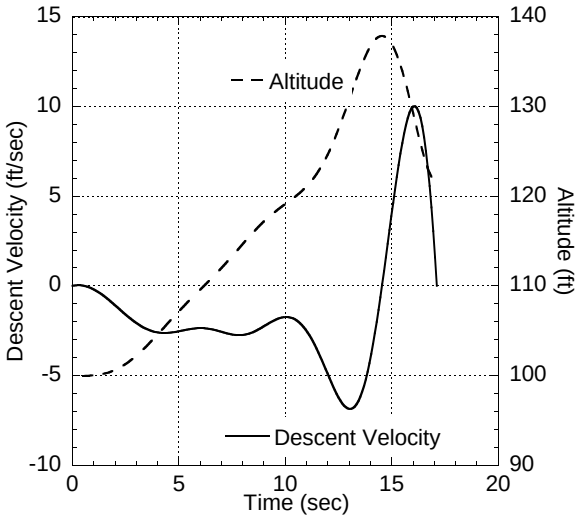

Fig. 13. Vertical speed and altitude for partial power flyaway transition to minimum power speed.

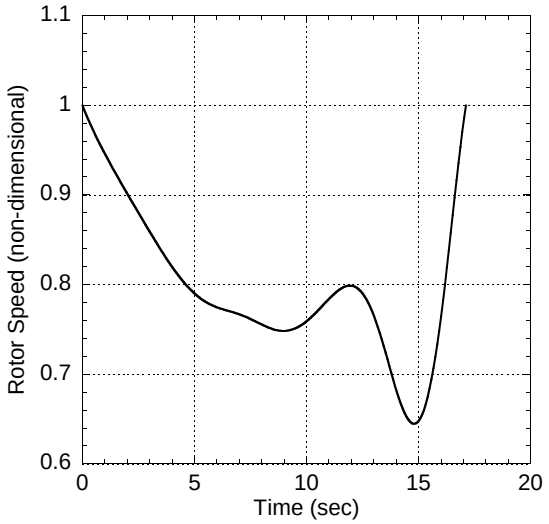

Fig. 14. Non-dimensional rotor speed for partial power flyaway transition to minimum power speed.

is important to note that no optimization has occurred. Only the constraint error has been eliminated.

The effect on rotor speed is shown in Figure 14. The reason for the high thrust coefficient is more clear considering that the rotor speed drops to about 65%. A significantly larger thrust coefficient is necessary for the same thrust at such a low rotor speed. But the decrease in thrust coupled with the rapid decrease in altitude causes the rotor speed to recover to 100% at the end of the analysis interval to meet the end constraint. In reality, a pilot would never allow rotor speed to go so low, and probably could not recover it if it did droop that much. But there is no constraint on rotor speed in the present implementation, so such large variations can occur in the simulated flight path.

This example illustrates how the optimal control meets all of the constraints placed on it, and how if it is not sufficiently constrained, will produce a flight path that is not physically reasonable. To obtain a flight path more representative of what a human pilot would fly will require modifications to the model. There are two paths to take. Either additional constraints must be placed, creating more burden for the single restoration, or the existing constraints can be relaxed and their effect achieved using the gradient phase to optimize the path. In the latter case, the gradient phase can improve the flight path over many gradient steps while the current implementation only allows one restoration phase.

Conclusions

An analysis for flyaway or descent to landing with power loss has been developed using optimal control to simulate the pilot reaction. The momentum theory vehicle model extends previous work by using rate controls and additional constraints on the optimal control procedure. Based on work to date, the following conclusions are offered.

1. Descent to landing and partial power flyaway have been considered. Suitable initial and end conditions for landing have been developed. Partial power flyaway is still in development and will require additional refinement to consistently obtain satisfactory flight paths.

2. For benign conditions, simple controls such as horizontal and vertical thrust coefficients or thrust coefficient and disk angle, are adequate controls.

3. Rate controls and additional constraints were found to adequately address specific deficiencies observed in the original analysis when a broad range of initial speeds and altitudes are tested, at the cost of additional analysis complexity.

4. For autorotation from a forward flight initial condition, the optimal control procedure-determined flight path agrees well with test data for a human-piloted autorotation.

5. For autorotation from hover, the analysis replicates the qualitative trends of the test data. By adjusting the objective function to approximate the horizontal touchdown speed in the test data, quantitative agreement could also be obtained.

References

[1]Johnson, W., "Helicopter Optimal Descent and Landing After Power Loss," NASA TM 73244, Ames Research Center, May 1977.

[2]Lee, A. Y., Bryson, A. E., Jr., and Hindson, W. S., "Optimal Landing of a Helicopter in Autorotation," *Journal of Guidance, Control, and Dynamics*, Vol. 11, (1), January–February 1988, pp. 7–12.

[3]Lee, A. Y.-N., *Optimal Landing of a Helicopter in Autorotation*, Ph.D. thesis, Stanford University, July 1985.

[4]Miele, A., Damoulakis, J. N., Cloutier, J. R., and Tietze, J. L., "Sequential Gradient-Restoration Algorithm for Optimal Control Problems with Nondifferential Constraints," *Journal of Optimization Theory and Applications*, Vol. 13, (2), 1974, pp. 218–255.

[5]Gessow, A. and Myers, G. C., *Aerodynamics of the Helicopter*, Frederick Ungar Publishing Company, New York, 1952.

[6]Cheeseman, I. C. and Bennett, W. E., "The Effect of the Ground on a Helicopter Rotor in Forward Flight," ARC R&M 3021, September 1955.

[7]Wood, T. L., "High Energy Rotor System," Preprint No. 1014, American Helicopter Society 32nd Annual National V/STOL Forum, Washington, D. C., May 10–12, 1976.

[8]Dooley, L. W. and Yeary, R. D., "Flight Test Evaluation of the High Inertia Rotor System," USARTL-TR 79-9, U.S. Army Research and Technology Laboratories (AVRADCOM), Fort Eustis, VA, June 1979.